Supporting Information

Preparation of $ZnCo_2O_4$@PANI core/shell nanobelts for high-performance asymmetric supercapacitors

Xiaobo Chen*, Jianghao Cai

School of New Energy and Electronic Engineering, Yancheng Teachers University, Yancheng, 224051, PR China

E-mail addresses: chenxbok@126.com

Experimental details

Structural characterizations

The X-ray diffraction (XRD) patterns recorded using a SHIMADZU XRD-6100 instrument with Cu-Kα radiation. The X-ray photoelectron spectra (XPS) were collected by a Thermo ESCALAB 250 electron spectrometer with an X-ray source of Al Ka. The scanning electron microscopy (SEM) imaging was conducted by Zeiss Supra 35VP scanning electron microscope, and the transmission electron microscopy (TEM) and high-resolution TEM (HRTEM) imaging was conducted by JEOL-2010 transmission electron microscope with 200 kV accelerated voltage. The specific surface area (BET method) of the samples were determined by nitrogen (N_2) adsorption/desorption using an ASAP 2020 V3.01 G instrument.

Electrochemical measurements

All electrochemical tests were carried out on a CHI660E electrochemical workstation with the Ni foam carrying active material as the working electrode, Pt wire as the counter electrode was, and AgCl/Ag as the reference electrode. Besides, the electrolysis was 2 M KOH aqueous solution (50 mL). The galvanostatic charge/discharge (GCD) test and cycling test were conducted using a LAND battery program-control test system (CT2001A).

All working electrodes were fabricated by mixing the active material, carbon black, and polyvinylidene fluoride with a mass ratio of 85:10:5 in the N-methyl

pyrrolidone (NMP) solvent. Subsequently, the mixture was coated onto nickel foam and dried in a vacuum oven at 60 °C for 2 h. The mass loading of the active material on Ni foam is about 5.5 mg cm^{-2}.

The specific capacity C_s (F g^{-1}) of $ZnCo_2O_4$ and $ZnCo_2O_4$@PANI electrodes is obtained from Equation (S1).

$$C_s = \frac{I\Delta t}{m\Delta V} \quad \text{(S1)}$$

where Δt (s) is the discharge time, I (A) is the applied current, m (g) is the is the loading mass of active material, ΔV is the discharge potential range.

To explore the reaction kinetics, we further analyzed the linear correlation of the peak current (i) and sweep rate (v) based on the following formula:

$$i = a \times v^b \quad \text{(S2)}$$

where (a, b) are constants, and the log (v) slope versus log(i) indicates the b-value which provides fundamental data about the charge storage kinetics.

The contribution ratio of capacitive and diffusion to the total charge storage can be determined from the CV curves using to the following equation, in which, $k_1 v$ stands for the capacitive controlled current and $k_1 v^{1/2}$ represents diffusion control process:

$$i(\mathrm{V}) = k_1 v + k_2 v^{1/2} \quad \text{(S3)}$$

Fabrication of asymmetric supercapacitor device

In a two electrode system, the asymmetric supercapacitor (ASC) device was constructed by using the $ZnCo_2O_4$@PANI as the positive electrode and AC as the negative electrode with a cellulose paper as the separator in 2 M KOH as electrolyte. Besides the capacity, charge balance between the cathode and anode also determines the ASC performance. To realize the charge balance, the active mass ratio of the cathode to anode was carefully decided according to the equation of $m_+/m_- = (C_-\Delta V_-)/(C_+\Delta V_+)$, where m_+ and m_- are the active masses, C_+ and C_- are the specific capacities obtained by the three-electrode test, and ΔV_+ and ΔV_- are the potential

windows of the cathode and anode, respectively. Based on the charge balance equation, the optimal mass loading of AC was estimated about 9.8 mg cm^{-2}.

The specific capacity C_{device} (C g^{-1}), specific energy E (Wh kg^{-1}) and specific power P (W kg^{-1}) of asymmetric supercapacitors can be calculated from the Equation (S2-S4), respectively.

$$C_{device} = I\Delta t/m \quad \text{(S4)}$$

$$E = \frac{\int_{t1}^{t2} IV_{(t)}dt}{m \times 3.6} \quad \text{(S5)}$$

$$P = 3600E/\Delta t \quad \text{(S6)}$$

where I (A) corresponds to the applied current, Δt (s) means the discharging time, m (g) represents the total loading mass of active materials on both cathode and anode, t_1 (s) is the initial time after IR drop, t_2 (s) is the final time of discharge, and $\int V(t)\mathrm{d}t$ is the integrated area of discharge curves after IR drop.

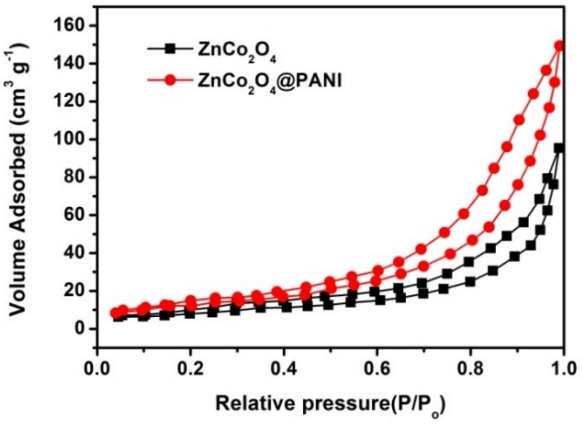

Fig. S1 Nitrogen adsorption-desorption isotherms of $ZnCo_2O_4$ and $ZnCo_2O_4$@PANI nanocomposite.

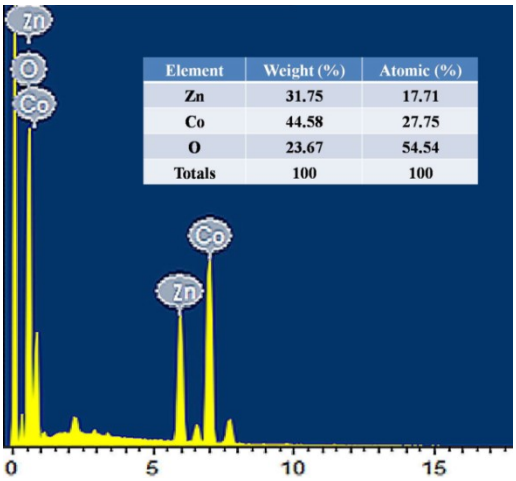

Fig. S2 The EDX spectrum of $ZnCo_2O_4$.

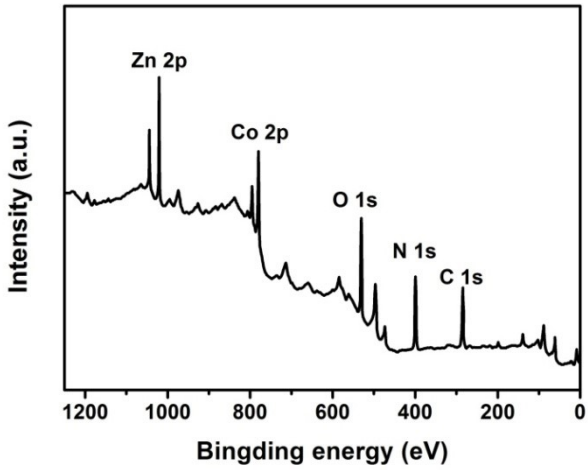

Fig. S3 Survey scan spectrum of $ZnCo_2O_4$/PANI.

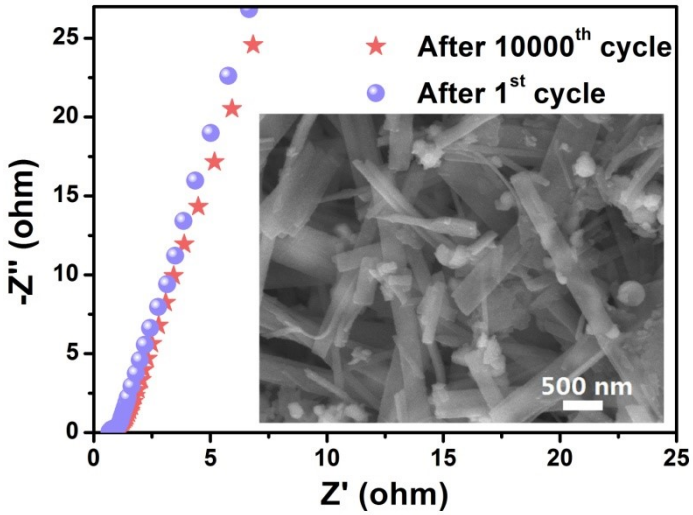

Fig. S4 Nyquist plots of the $ZnCo_2O_4$@PANI before and after 10000 cycles and SEM image (inset) of $ZnCo_2O_4$@PANI after 10000 cycles.

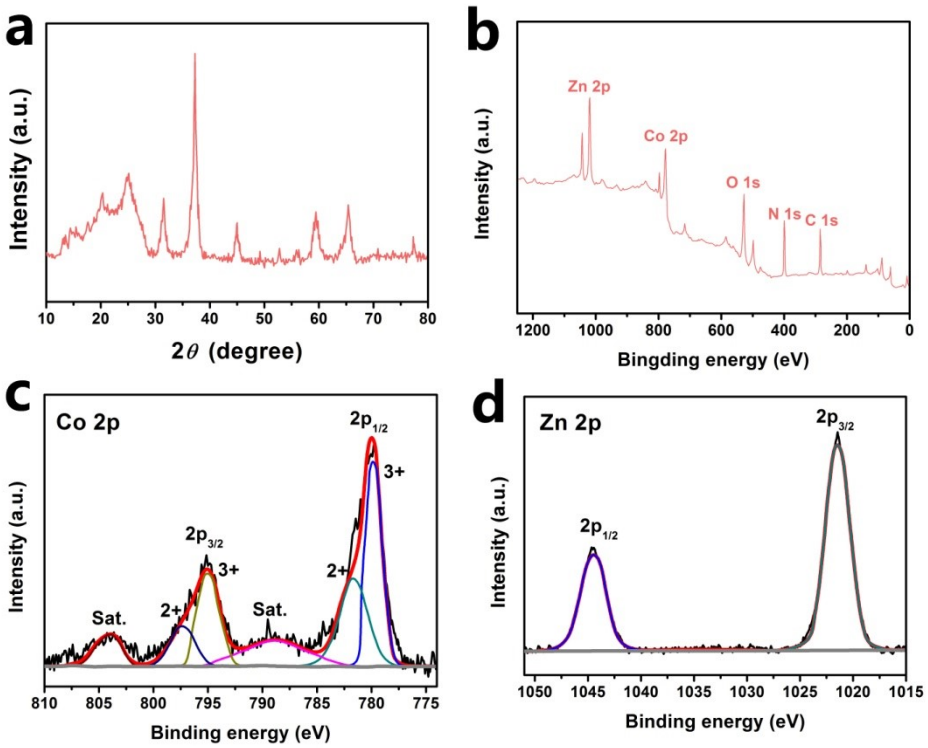

Fig. S5 (a) XRD pattern of after 10000 cycles. (b-d) XPS spectra of after stability test.

Table S1. Comparison of electrochemical performance of $ZnCo_2O_4$@PANI electrode with previously reported $ZnCo_2O_4$-based electrodes.

Materials	Specific capacitance (C g^{-1})	Capacitance retention (%)	Cycling stability (%) (current, cycles)	Ref.
$ZnCo_2O_4$ quasi-cubes	804 F g^{-1} at 1 A g^{-1}	74.5% at 16 A g^{-1}	79.2% after 3000 cycles at 5 A g^{-1}	[1]
hexagonal-like $ZnCo_2O_4$	845.7 F g^{-1} at 1 A g^{-1}	57.6% at 5 A g^{-1}	95.3% after 5000 cycles 5 A g^{-1}	[2]
$ZnCo_2O_4$ nanoparticles	843 F g^{-1} at 1 A g^{-1}	72.7% at 3 A g^{-1}	97% after 5000 cycles at 1 A g^{-1}	[3]
$ZnCo_2O_4$ nanoflakes	311.26 mAh g^{-1} at 1 A g^{-1}	60.4% at 15.0 A g^{-1}	\	[4]
OV- $ZnCo_2O_4$ nanosheets	2111 F g^{-1} at 1 A g^{-1}	62.15% at 32 A g^{-1}	95.5% after 4000 cycles	[5]

Materials	Specific capacitance ($C\ g^{-1}$)	Capacitance retention (%)	Cycling stability (%) (current, cycles)	Ref.
$ZnCo_2O_4$/NF	1143 F g^{-1} at 1.25 A g^{-1}	65.4% at 12.5 A g^{-1}	103% after 6000 cycles at 12.5 A g^{-1}	[6]
$ZnCo_2O_4$ nanowires	776.2 F g^{-1} at 1 A g^{-1}	\	84.3% after 1500 at 3 A g^{-1}	[7]
$ZnCo_2O_4$@N-GO/PANi	720 F g^{-1} at 1.5 A g^{-1}	\	~96.4% after 10000 cycles	[8]
leaf-like ZnCo2O4	1700 F g^{-1} at 1 A g^{-1}	\	110% after 8000 cycles	[9]
$ZnCo_2O_4$@PANI core/shell nanobelts	1938.2 F g^{-1} at 1 A g^{-1}	88.6% at 10 A g^{-1}	92.4% after 10000 cycles at 6 A g^{-1}	This work

Table S2. A comparison on the specific capacitance, specific energy, specific power and electrolyte of $ZnCo_2O_4$@PANI//AC ACS with the previously reported ASCs devices.

Electrode material	Specific capacity at current density	Specific energy (Wh kg^{-1})	Specific power (W kg^{-1})	Cycle Performance	Ref.
Au@rGO-$ZnCo_2O_4$//AC	113.8 F/g at 10 mA/cm^2	31	2121	97.1% after 5000 cycles	[10]
$ZnCo_2O_4$ QCs//AC	85.72 F g^{-1} at 1 A g^{-1}	34.4	860.1	112.4% after 3000 cycles at 5 A g^{-1}	[1]
$ZnCo_2O_4$ nanoparticles//AC	90 F g^{-1} at 1 A g^{-1}	26.28	716	90% at 5000 cycles at 5 A	[3]

Electrode material	Specific capacity at current density	Specific energy (Wh kg^{-1})	Specific power (W kg^{-1})	Cycle Performance	Ref.
				g^{-1}	
$ZnCo_2O_4$ nanoflakes//AC	59.6 F g^{-1} at 1 A g^{-1}	21.2	800	93.2% 10,000 cycles at 5 A g^{-1}	[4]
OV-$ZnCo_2O_4$ nanosheets//AC	97.4 F g^{-1} at 0.2 A g^{-1}	34.6	160	93% after 3000 cycles at 2 A g^{-1}	[5]
$ZnCo_2O_4$//F-RGO	229 F g^{-1} at 0.25 A g^{-1}	84.48	400	\	[7]
leaf-like $ZnCo_2O_4$//AC	170 F g^{-1} at 1 A g^{-1}	63	795.5	98% after 4000 cycles at 2 A g^{-1}	[9]
$ZnCo_2O_4$@PANI//AC	187.3 F g^{-1} at 1 A g^{-1}	66.6	800.1	92.5% after 10000 cycles at 8 A g^{-1}	This work

References

[1] H. Chen, X. Du, J. Sun, H. Mao, R. Wu, C. Xu, Simple preparation of $ZnCo_2O_4$ porous quasi-cubes for high performance asymmetric supercapacitors, Applied Surface Science 515 (2020) 146008.

[2] V. Venkatachalam, A. Alsalme, A. Alswieleh, R. Jayavel, Double hydroxide mediated synthesis of nanostructured $ZnCo_2O_4$ as high performance electrode material for supercapacitor applications, Chemical Engineering Journal 321 (2017) 474-483.

[3] J. Bhagwan, S.K. Hussain, J.S. Yu, Aqueous asymmetric supercapacitors based on $ZnCo_2O_4$ nanoparticles via facile combustion method, Journal of Alloys and Compounds 815 (2020) 152456.

[4] J.-H. Eum, D. Mandal, H. Kim, A novel synthesis of 2D porous $ZnCo_2O_4$ nanoflakes using deep eutectic solvent for high-performance asymmetric supercapacitors, Journal of Electroanalytical Chemistry 892 (2021) 115299.

[5] K. Xiang, D. Wu, Y. Fan, W. You, D. Zhang, J.-L. Luo, X.-Z. Fu, Enhancing bifunctional electrodes of oxygen vacancy abundant $ZnCo_2O_4$ nanosheets for supercapacitor and oxygen evolution, Chemical Engineering Journal 425 (2021) 130583.

[6] H.S. Jadhav, A. Roy, W.-J. Chung, J.G. Seo, Growth of urchin-like $ZnCo_2O_4$ microspheres on nickel foam as a binder-free electrode for high-performance supercapacitor and methanol electro-oxidation, Electrochimica Acta 246 (2017) 941-950.

[7] L. Xu, Y. Zhao, J. Lian, Y. Xu, J. Bao, J. Qiu, L. Xu, H. Xu, M. Hua, H. Li, Morphology controlled preparation of $ZnCo_2O_4$ nanostructures for asymmetric supercapacitor with ultrahigh energy density, Energy 123 (2017) 296-304.

[8] A. Kathalingam, S. Ramesh, H.M. Yadav, J.-H. Choi, H.S. Kim, H.-S. Kim, Nanosheet-like $ZnCo_2O_4$@nitrogen doped graphene oxide/polyaniline composite for supercapacitor application: effect of polyaniline incorporation, Journal of Alloys and Compounds 830 (2020) 154734.

[9] L. Cheng, M. Xu, Q. Zhang, G. Li, J. Chen, Y. Lou, NH4F assisted and morphology-controlled fabrication of $ZnCo_2O_4$ nanostructures on Ni-foam for enhanced energy storage devices, Journal of Alloys and Compounds 781 (2019) 245-254.

[10] S.J. Patil, D.P. Dubal, D.-W. Lee, Gold nanoparticles decorated rGO-$ZnCo_2O_4$ nanocomposite: A promising positive electrode for high performance hybrid supercapacitors, Chemical Engineering Journal 379 (2020) 122211.